scientific reports

Check for updates

OPEN

Gazing into spatiotemporal 'known unknowns': the influence of uncertainty on pupil size and saccadic eye movements

Aïcha Boutachkourt[1,2], Dominika Drążyk[1] & Marcus Missal[1]✉

Expectation of a future stimulus increases the preparedness to act once it actually appears and results in reduced latency of the appropriate motor response. Real world events are uncertain both spatially and/or temporally but this uncertainty could itself be expected. In the presence of both expected spatial and temporal uncertainty, which one should be prioritized by the motor system could depend on the context. Therefore, we investigated the relative weight of expected spatial and temporal uncertainty during the preparation of a saccadic eye movement. A reaction time task was used with a variable foreperiod between a warning and an imperative visual stimuli. Expected temporal and/or spatial uncertainty associated with the stimulus was cued. We found that before imperative stimulus onset, pupil dilation increased with expected temporal uncertainty but was unaltered by spatial uncertainty. After imperative stimulus onset, both types of expected uncertainty affected saccade latency. Maximum eye velocity was modulated by expected spatial uncertainty only. In conclusion, expected temporal and spatial uncertainty do not have the same impact on preparation and execution of a motor response. There could be a prioritization of the relevant information as a function of the evolving expected uncertainty context during the task.

Keywords Temporal uncertainty, Spatial uncertainty, Expectation, Pupil dilation, Saccadic eye movements

From the simplest to the most complex activities, the brain constantly forms expectations about future events. 'Expectation' is generally defined as the preparation of sensorimotor and cognitive systems for the future occurrence of a particular stimulus. This preparation is based on prior information about regularities present in a given context[1,2] and could be conceptualized as a narrowing down of the spatiotemporal probability space of the future stimulus[3]. However, future events are uncertain and always accompanied by some degree of expected spatial and/or temporal 'uncertainty'. These two forms of uncertainty could also be referred to as 'known unknowns'. In order to produce an optimal behavioral response, expected uncertainty should be estimated and could impact movement preparation and execution[4,5].

The influence of temporal uncertainty on movement preparation can be estimated using the simple variable foreperiod paradigm ('vFP'[6,7]; for a modern synthesis see[8]). The vFP paradigm consists of the appearance of only two stimuli: a warning stimulus (further abbreviated as 'WS'; e.g. a sound or a visual flash) and an imperative stimulus ('IS'; e.g. a target on a computer display), separated by a delay called the foreperiod ('FP'). The WS allows the subject to prepare for an upcoming IS that requires a quick motor response. Changing the probability distribution of FP duration affects temporal expectation of the IS[9,10] and therefore modulates motor responses. Motor responses (most often a button press) have a shorter latency when the probability of IS occurrence is higher[7,10–14]. This effect has also been observed in the oculomotor domain in primates[15,16] and humans[17–22]. Given that the influence of elapsed time on motor preparation during the FP occurs without participants being informed about the temporal aspect of the task, it could be qualified as being implicit in most foreperiod effect studies[17]. However, explicit visual cues could also be used to provide prior information about the duration of the FP and to allow for optimal allocation of attentional resources to the timing of the future stimulus[21,23–26]. Expectation is often estimated by measuring reaction times, but pupil dilation could also be used as a proxy measure of temporal preparation[27].

[1]Institute of Neurosciences (IONS), Cognition and System (COSY), Université Catholique de Louvain, 53 Av Mounier, B1.53.04 COSY, 1200 Brussels, Belgium. [2]Neuropsychiatry, Department of Neurosciences, Leuven Brain Institute, KU Leuven, Leuven, Belgium. ✉email: marcus.missal@uclouvain.be

Pupil size could reflect changes in both temporal and spatial expectations[28,29]. The influence of expected spatial uncertainty on movement preparation and execution can be tested by providing experimental subjects with a probabilistic cue. For instance, a cue could inform subjects that the IS could occur at only one position (no uncertainty) or at one of several likely positions. Using this approach, Drążyk and Missal[22] found that the latency of visually-guided saccades increased with increasing expected spatial uncertainty. Furthermore, maximal pupil dilation and maximum saccadic velocity (further abbreviated 'V_{max}') were observed when there was no spatial uncertainty[22].

To our knowledge, most previous studies of expected uncertainty have focused either on temporal or spatial uncertainty, separately. However, perceptual events in everyday life are associated with expected spatial and temporal uncertainty—together. Expected uncertainty about future events in a more realistic context must incorporate these two sources of uncertainty[4]. Indeed, humans perceive sensory events globally with various features bound together (as suggested by 'Gestalt laws of perceptual organization'; see[30]). Perhaps various sources of uncertainties could also be bound together (expected 'combined' uncertainty). In agreement with this hypothesis, an improved behavioral performance due to temporal expectation in a visual discrimination task was observed only in conditions where the future location of the target was known and therefore totally predictable[31]. In contrast, a more recent study showed no behavioral effects related to the combination of spatial attention and contextual temporal expectation in a reaction time task[32].

The goal of the present study was to determine how expected spatial and temporal uncertainty could interact and how this could affect pupil size as well as the preparation and execution of saccadic eye movements.

Methods

Subjects and ethics

This study was conducted at the Université catholique de Louvain, Belgium. Participants were volunteers (18–65 years old) with normal or corrected to normal vision and did not suffer from any known neurological or psychiatric diseases. Subjects declared not to take psychoactive substances at least a day before the experiment. Thirty subjects (*average* ± *sd*, age 24.57 ± 8.14 years, 16 women) provided their informed written consent and took part in this study. All procedures were conducted in accordance with the Declaration of Helsinki guidelines and approved by the Ethics Committee of the Université catholique de Louvain under number B403201733677. Data is available to participants upon written request.

Experimental design

The present study is based on an oculomotor variant of the classic variable foreperiod paradigm[7]. Each trial started with the appearance of a fixation dot at the bottom of the screen for 500 ms ('fixation period', see Fig. 1A). Next, two types of cues appeared on the screen ('cue period'). The spatial cue consisted of three circular empty disks (referred to as 'placers') regularly spaced from the left to the right side of the screen. Each placer circumference could appear either as red or white. If one placer was red, the future position of the IS was certain and therefore there was no spatial uncertainty (condition 'S_{U1}', see Fig. 1A). If two placers were red, the future IS could appear at one of these two positions with the same probability (increased expected spatial uncertainty, 'S_{U2}'). Finally, when all three placers were red, expected spatial uncertainty was maximal ('S_{U3}'). The temporal cue consisted in a star-like shape, located at the bottom of the screen at the place of the fixation dot. The star shape could have one of three different numbers of branches. A star with 3 branches indicated that the IS could appear after 1525 ms (23.33% of trials marked by this star), 1600 ms (53.33% of trials) or 1675 ms (23.33% of trials, see Fig. 1B). This distribution assumed the FPs to last on average 1600 ± 75 ms (*mean* ± *sd*) and set up a context of minimal temporal uncertainty (condition 'T_{U1}'; kurtosis = 2.14; referred to as 'leptokurtic'). The five-arm star cued a wider FP distribution: the IS could appear after 1250 ms (25.55% of trials marked by this star), 1600 ms (48.88% of trials) or after 1950 ms (25.55% of trials; 1600 ± 350 ms; condition 'T_{U2}'; kurtosis = 1.96; 'mesokurtic'). Finally, the nine-arm star shape indicated a flatter distribution: IS could occur after 975 ms (32.22% of trials marked by this star), 1600 ms (35.55% of trials) or after 2225 ms (32.22% of trials, 1600 ± 625 ms; condition 'T_{U3}'; kurtosis = 1.55; 'platykurtic'). Expected temporal uncertainty increased as: $T_{U1} \rightarrow T_{U2} \rightarrow T_{U3}$. In summary, the increasing kurtosis of the distribution was cued to subjects with an increasing number of branches of the star shape. Increasing the kurtosis of the IS distribution increased expected temporal uncertainty.

During each trial, subjects were asked to maintain gaze on the star shape while memorizing the position of the red placers in the periphery. After 2000 ms, all placers turned white and the temporal cue was replaced with a fixation dot for 500 ms. Next, a warning stimulus ('WS', a smiling face) appeared on top of the fixation dot for 50 ms. The disappearance of the WS marked the beginning of the 'foreperiod' ('FP'). At the end of the FP the imperative stimulus ('IS', same face) appeared in one of the previously red labeled placers. The task of the subject was to make a saccadic eye movement towards the IS as quickly as possible. If saccadic latency was less than 400 ms, subjects received a positive feedback (a score point, indicated by the '+1' text on the screen, see Fig. 1A).

The experiment consisted of 9 unique pairings of spatial and temporal uncertainty (3 T_U levels × 3 S_U levels). Each pairing was repeated 30 times in randomized order. Therefore, the testing phase of the experiment consisted of a total of 270 trials distributed into 9 blocks of equal length. After each block, a short rest period was interleaved and eye-tracker calibration was performed.

Trials were also grouped a posteriori into four categories referred to as 'combined uncertainty' ($Comb_U$): 'min.$_U$' included all trials with minimal spatial (S_{U1}) and temporal (T_{U1}) expected uncertainty; 'max.S_U' represented all trials with maximal spatial (S_{U3}) but minimal temporal (T_{U1}) uncertainty; 'max.T_U' included all trials with maximal temporal (T_{U3}) but minimal spatial (S_{U1}) uncertainty; 'max.$_U$' incorporated all trials with maximal spatial (S_{U3}) and temporal (T_{U3}) expected uncertainty. Given the a posteriori nature of this grouping, it will be used only as an hypothesis and a suggestion for further studies.

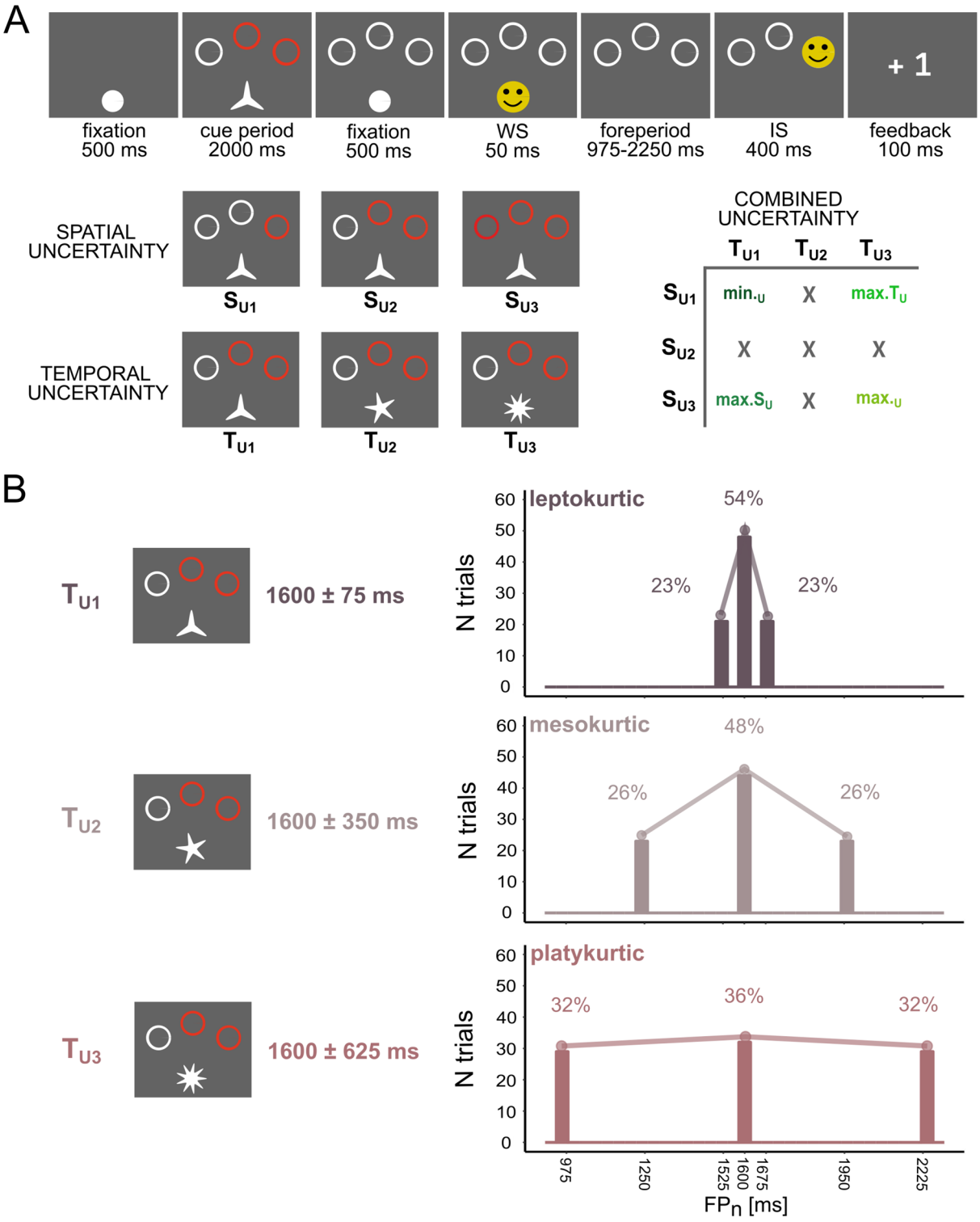

Figure 1. Schematic representation of the experimental design. (**A**) Each trial started with a 'fixation period' during which the gaze had to be oriented on a dot at the bottom of the screen. Next, during the 'cue period', spatial ('*placers*') and temporal cues ('*star*') were presented. Subjects were asked to maintain gaze on the star shape while memorizing the position of the red placers. Red placers indicated the possible location of the future IS. Next, a warning stimulus ('WS', smiley face) was briefly presented on the screen for 50 ms. Its disappearance indicated the beginning of the 'foreperiod' or FP. At the end of the FP, the imperative stimulus ('IS', second smiley) appeared at one of the cued positions for 50 ms. Subjects were asked to make a saccade towards the second smiley as quickly as possible. If saccadic latency was < 400 ms, subjects received positive feedback ('+1'). The *star shape* cue indicated the level of expected temporal uncertainty. Besides testing for the interaction between the S_U and T_U variables, a posteriori grouping of trials into four different categories referred to as 'combined uncertainty' ($Comb_U$) was implemented. $Comb_U$ corresponds to extreme cases in the experimental matrix. (**B**) Foreperiod distributions with different kurtosis used to create three levels of temporal uncertainty. The three-arm star (T_{U1}, leptokurtic) indicated that the IS may occur with low temporal uncertainty. The five-arm star (T_{U2}, mesokurtic) indicated a higher level of expected temporal uncertainty whereas the nine-arm star (T_{U3}, platykurtic) indicated maximal expected temporal uncertainty.

In order to maintain the motivation of subjects during the experiment, a score point was granted for each saccade directed towards the smiley and executed quickly enough. Furthermore, in 25% of trials (randomly), the IS did not appear at the end of the FP (referred to as 'catch trials'). Catch trails were used to keep the attentional level of subjects high. Subjects could still obtain a score point in catch trials by making a saccade towards any placer with a latency < 400 ms. Separate statistical analysis was also conducted on the latency and V_{max} of saccades executed during catch trials.

Training session

The experimental session started with a set of training blocks. The first stage consisted of 6 trials that familiarized subjects with the three spatial uncertainty conditions (S_{U1}, S_{U2} and S_{U3}). During this stage of training, FP duration was kept constant (1600 ms). The second stage consisted of 150 trials divided into three blocks, each block with one temporal cue. Only one red placer was presented (S_{U1} condition) and subjects focused on forming a mapping between the star shape and the kurtosis of the FP distribution. Finally, the last stage consisted of 9 trials with all cue pairings presented together in different trials randomly.

Each step of the training procedure was preceded by a verbal explanation of the meaning of each cue. Subjects were informed that the red placers provided information about the future location of the IS and that the star shapes carried information about the expected timing of the IS. No explanation was provided concerning the exact shape of the distributions and subjects were not informed about the presence of catch trials.

Data collection and preprocessing

Procedures for displaying stimuli and recording eye movements were created with Experimental Builder (SR Research, Mississauga, Ontario). Binocular eye movements were digitized at 500 Hz with an EyeLink1000 (SR Research, Mississauga, Ontario). The eye tracker was calibrated at the beginning of each data collection session and re-calibrated every 30 trials (before each new block). Subjects were sitting at a distance of 80 cm from the high resolution screen (size: 54 × 30 cm, 1920 × 1080 pixels, VPixx Technologies, Canada) displaying stimuli at 60 Hz.

Artefact rejection was conducted with DataViewer (SR Research, Ontario, Canada) to exclude oculomotor recordings of poor quality. Trials with frequent blinking, discontinuous recording or drift of calibration were excluded from further analysis. Rejection amounted to 9.54% of all trials only. Saccades were detected using an amplitude (> 1°), velocity (> 22°/s) and acceleration (> 3800°/s^2) criteria. Only visually-guided saccades initiated between 100 and 400 ms after IS onset and landing within the IS placer were further analyzed (53.57% of all trials). If an early saccade was detected during the foreperiod (13.49% of all trials), or the trial was a 'catch', data was not included in the final analysis. After outlier rejection there were on average 140 ± 36 latency and 137 ± 37 V_{max} data points per subject included in the final analysis.

Saccades can be a source of the pupillometry artifacts[33]. Therefore, two preprocessing steps were applied to the pupil size data set. Firstly, pupil analysis during the FP was conducted only for the longest possible interval that did not include IS onset ('IS-free interval'). This interval was equal to the shortest possible FP of 975 ms (see Fig. 1). Secondly, trials including any early saccade executed during the FP were excluded from the pupil data analysis. Pupil diameter recorded during this IS-free interval was then downsampled to 100 Hz and further processed in R using the PupilPre library[34]. Pupillary responses from the left and the right eye were averaged on the trial-by-trial basis to improve the stability of the signal. Periods of lost data caused by a blink were replaced with a linear interpolation based on pupil size before and after the event. Next, pupil size during the baseline period (starting 200 ms before and ending at the onset of the FP) was subtracted from the data. Finally pupil traces were normalized using z-score[35]. After preprocessing there were on average 143 ± 39 pupil responses per subject included in the final analysis.

Statistical analysis

To minimize the multiple comparison problem related to the continuous character of the signal, the pupillary response was first analyzed using a cluster-based permutation test ('CBPT',[36]). In CBPT, a chosen test statistic is first computed and thresholded on the original time series. Afterwards, time series were shuffled and the test was repeated *n* times ('permutation') to simulate the null distribution of the test statistic. Finally, the test statistic of the original time series was compared to the distribution of permuted test statistics. P-values calculated from this comparison were then thresholded using the significance level assumed in this study (0.01). The raw pupil signal was subjected to CBPT analysis in R using the 'permutes' package[37]. A Linear Mixed Model version of the permutation test was used, with the subject's identifiers as random intercept. To assess the main effect of the model, the permutation type 'anova' was chosen and 1000 permutations were performed. The CBPT approach was used in order to find a time cluster of potential difference in pupillary response for different experimental conditions. Once the analysis established a final cluster of significance (expressed as a millisecond time range), data from that cluster was averaged on the trial-by-trial basis[38] and tested with type II ANOVA ('car' package version 3.1-2[39]).

Latency and V_{max} were fitted using a Linear Mixed Model (LMM, 'lme4' package version 1.1-30[40]). As the LMM models used Gaussian distribution and the data spread for no-catch trials was right-skewed, saccadic latencies were log-transformed. Due to the normal distribution of data values in catch trials, their analysis was conducted without logarithmic transformation of the saccadic latency. The quality of models was examined using QQplots and residuals (package 'performance'[41]). Models used the following predictors: 'T_U'—level of expected temporal uncertainty cued in the given trial; 'S_U'—level of expected spatial uncertainty The following labeling of models was used: the 'full' prefix indicated the model with maximal fixed effect structure. Models including only one predictor were labeled using the name of the used predictor (e.g. 'S_U'). Further, the random structure of models was denoted using the 'rs' suffix and the consecutive number. For example: 'S_U.rs1' denotes

a model with S_U as predictor and a random intercept structure; 'S_U.rs2' denotes a model with S_U as predictor and random slope structure.

Full LMM models were first fitted using the restricted maximum likelihood method (REML[42,43]) and their Bayes Information Criterion was estimated (BIC[44]). The BIC of different models were compared to choose an optimal random term structure. For all full models, a random intercept structure performed better than the random slope (see Supplementary Table S1). Therefore, models with a random intercept structure and different predictors were re-fitted using a maximum likelihood method (ML). The BIC of each model was then recalculated and compared once more to find the best set of data predictors. Statistics of the best fitted model were then calculated (REML method) and presented in the "Results" section. Diagnostics of each of the presented models were evaluated to assure the quality of convergence and accordance with assumptions.

Results

The aim of the present study was to test whether expected temporal and spatial uncertainties interact and could have the same impact during movement preparation and execution.

Pupil size during the foreperiod

The influence of temporal and spatial expected uncertainty during the foreperiod ('FP') between the warning ('WS') and imperative stimuli ('IS') were estimated using pupil size as a behavioral indicator (see Fig. 2A for the impact of spatial uncertainty or 'S_U' and Fig. 2C for the impact of temporal uncertainty or 'T_U' in saccade-free intervals; longer traces of the pupillary response are presented in Fig. S1 of Supplementary Material). The time course of pupil size during the FP suggests that pupil dynamics during the first 500 ms was probably related to changes in luminance caused by the offset of the WS[33]. This interval from 0 to 500 ms was therefore excluded from the cluster-based permutation test (CBPT) analysis. A modulation of pupil size by expected spatial uncertainty ('S_U') was detected in the 500–930 ms range (CBPT method, $p_{mass} = 9.9 \times 10^{-4}$). This period will be referred to as the '$FP_{cluster}$.' This $FP_{cluster}$ was selected for further analysis using ANOVA and averaged on a trial-by-trial basis. However, the LMM analysis suggests that the difference of pupil size for different S_U levels during the $FP_{cluster}$ was too small to reach statistical significance ($p = 0.058$, see Fig. 2B; sample sizes: 45 ± 13 pupil responses per subject in S_{U1}, 50 ± 14 in S_{U2} and 48 ± 14 in S_{U3} condition).

A significant modulation of pupil size by temporal uncertainty ('T_U') was found during a period from 500 to 970 ms after WS offset (CBPT; $p_{mass} = 9.9 \times 10^{-4}$, see Table 1). The LMM analysis included 48 ± 13 of pupil responses per subject in T_{U1}, 48 ± 14 in T_{U2} and 47 ± 13 in T_{U3} condition. A significant main effect of T_U was found (ANOVA, $F^2 = 11.747$, $p = 8.17 \times 10^{-6}$). Within the $FP_{cluster}$, pupil size was larger in the T_{U3} compared to the T_{U2} ($p = 0.003$) and T_{U1} conditions ($p = 6.77 \times 10^{-6}$, Tukey post-hoc analysis, see Fig. 2D and Supplementary Table S2 online). This indicated that the pupillary response encoded only T_U about the future IS during the FP.

The LMM analysis included 15 ± 5 pupil responses per subject in min.$_U$, 17 ± 5 in max.S_U, 15 ± 5 in max.T_U and 16 ± 5 in max.$_U$ condition.

The possibility of interaction between temporal and spatial uncertainty on pupil size was also explored. A significant cluster of difference for the interaction ($S_U \times T_U$) was detected in the 500–970 ms range (CBPT method, $p_{mass} = 9.9 \times 10^{-4}$, see Table 1). However, a further LMM analysis suggests that the interaction effect in the specified cluster was too small to reach statistical significance ($p = 0.282$, see Table 1).

The temporal uncertainty $FP_{cluster}$ window was also used to average the pupillary traces for different levels of combined uncertainty ($Comb_U$, see Fig. 2E). Visual inspection of averaged responses suggest a general trend of increasing pupil dilation with $Comb_U$ (see Fig. 2F). However, this observation should be confirmed by further studies, given the *a posteriori* creation of the $Comb_U$ variable.

Latency of saccades

After the appearance of the IS, subjects were required to make a saccadic eye movement towards its spatial position as quickly as possible. To test the influence of different levels of spatial and temporal expected uncertainty on saccadic latency, a LMM was applied. Of all tested models, the 'full.rs1' model that incorporated the effect of spatial and temporal uncertainty as well as their interaction was best fitting the data (see Supplementary Table S1 online). However, despite the presence of a main effect, no interaction between spatial and temporal uncertainty was found ($p = 0.864$, see full.rs1 model in Table 2). This indicates that each type of uncertainty had its own independent effect on the measured outcome.

The LMM analysis included 45 ± 12 saccadic latencies per subject in S_{U1}, 48 ± 13 in S_{U2} and 46 ± 12 in S_{U3} condition. Spatial uncertainty strongly influenced saccadic latency ($p < 2.22 \times 10^{-16}$, see full.rs1 model in Table 2). Post-hoc Tukey comparisons showed that latency significantly increased between S_{U1} and S_{U2} ($p = 3.30 \times 10^{-14}$), S_{U1} and S_{U3} ($p < 2.22 \times 10^{-16}$) and S_{U2} and S_{U3} levels ($p = 1.71 \times 10^{-6}$, see Supplementary Table S3 online). Increasing spatial uncertainty influenced movement preparation and the latency of saccadic responses (see Fig. 3A).

The LMM analysis included 48 ± 12 saccadic latencies per subject in T_{U1}, 47 ± 14 in T_{U2} and 45 ± 12 in T_{U3} condition. The analysis showed a main effect of temporal uncertainty on saccadic latency ($p < 2.22 \times 10^{-16}$, see Table 2). Post-hoc Tukey comparisons indicated that the latency of saccades significantly increased between T_{U1} and T_{U3} ($p < 2.22 \times 10^{-16}$) and T_{U2} and T_{U3} levels ($p = 3.62 \times 10^{-14}$, see Supplementary Table S3 online). Increasing temporal uncertainty generally increased the latency of responses but the effect was not detected between the T_{U1} and T_{U2} levels (see Fig. 3B). Figure 3C suggests that increasing combined uncertainty strongly increased the latency of responses. Temporal and spatial uncertainty had a comparable and perhaps additive impact on the saccadic latencies (see Fig. 3C).

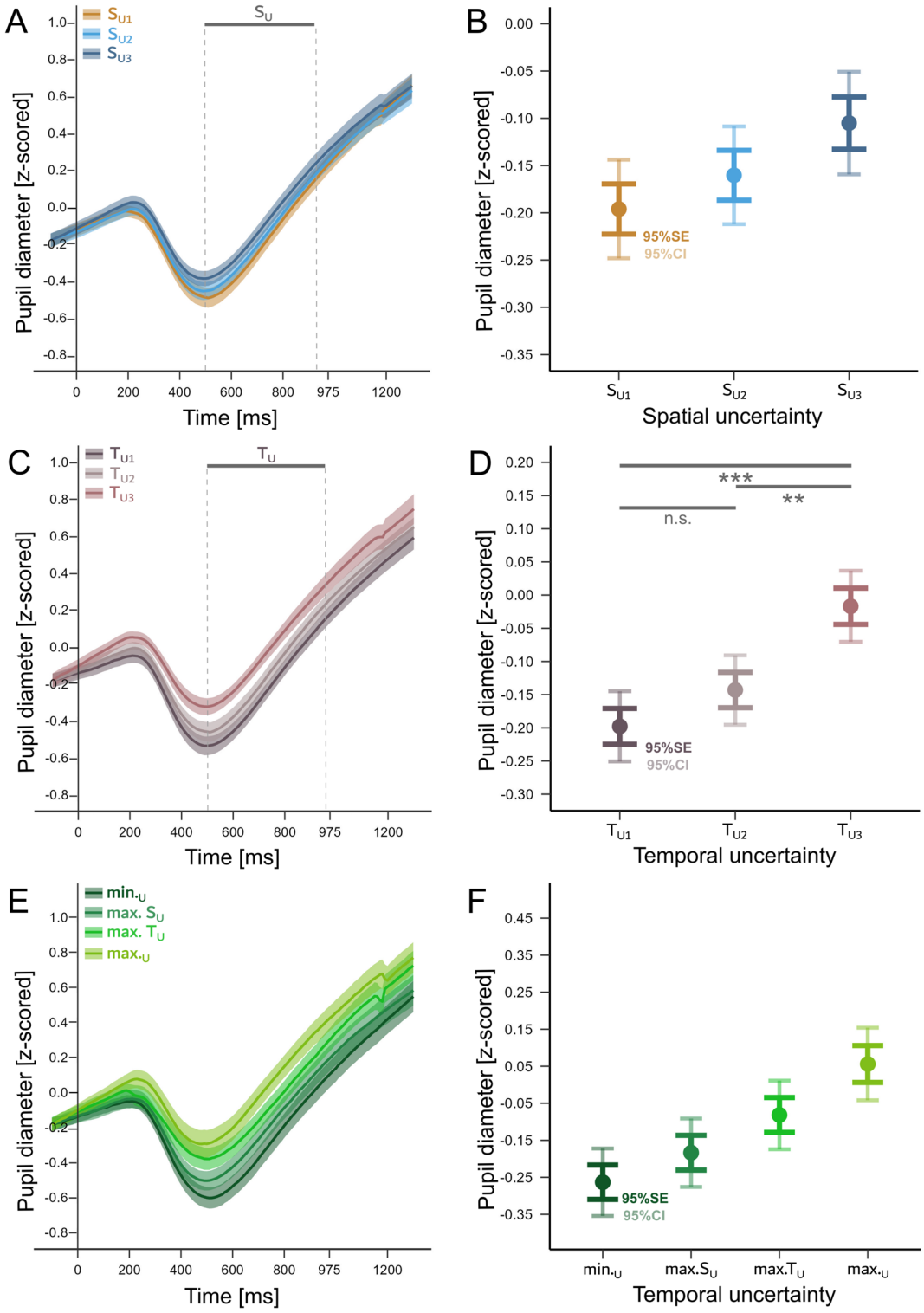

Figure 2. Pupillary responses during the foreperiod for different levels of expected uncertainty. (**A**) Time course of pupil size during the FP. Time 'zero' on the X-axis indicates the extinction of the warning stimulus. Colored lines indicate baseline corrected and z-scored mean pupil size in the different S_U conditions. The *horizontal gray line* indicates the cluster of significance detected using CBPT. (**B**) Pupil size averaged within the $FP_{cluster}$ (dot) for different levels of temporal uncertainty. Whiskers represent standard error (95% SE) and confidence intervals (95% CI). (**C**) Time course of pupil size during the FP. *Colored lines* indicate baseline corrected and z-scored mean pupil size in the different T_U conditions. (**D**) Pupil size averaged within the $FP_{cluster}$ (dot) for different levels of temporal uncertainty. *Horizontal black lines* indicate post-hoc significance between factor levels. Abbreviations: n.s. not significant, * $p < 0.01$, ** $p < 0.001$, *** $p < 0.0001$. (**E**) Time course of pupil size during the FP. *Colored lines* show the baseline corrected and z-scored mean pupil size in the different $Comb_U$ conditions. (**F**) Pupil size averaged within the T_U $FP_{cluster}$ (dot) for different levels of combined uncertainty. For combined uncertainty, only the general trend will be presented given that this variable was created retrospectively and that no planned comparisons could therefore be performed.

Method	CBPT			ANOVA		
Fixed terms	t_{mass} value	p_{mass} value	cluster	F value	df	p value
S_U	620.957	9.9×10^{-4}	500–930 ms	2.852	2	0.058
T_U	2243.267	9.9×10^{-4}	500–970 ms	11.747	2	8.17×10^{-6}
$S_U \times T_U$	917.648	9.9×10^{-4}	500–970 ms	1.263	4	0.282

Table 1. Statistical analysis of the influence of spatial and temporal uncertainties and their interaction on pupil size. Mass statistics were calculated by CBPT to establish a cluster of significant differences in milliseconds. Pupil size was averaged in that cluster and was further analyzed with a Type II ANOVA. *CBPT* cluster based permutation test, t_{mass} summed t statistics, p_{mass} p value for a cluster, *df* degrees of freedom.

Model	Outcome	Fixed terms	df	F value	p value	Random terms	σ
full.rs1	latency	S_U	2	76.143	$< 2.22 \times 10^{-16}$	subject	0.093
		T_U	2	88.157	$< 2.22 \times 10^{-16}$	residual	0.222
		$S_U * T_U$	4	0.320	0.864		
full.rs1	V_{max}	S_U	2	15.450	2.07×10^{-7}	subject	55.166
		T_U	2	0.749	0.473	residual	66.572
		$S_U * T_U$	4	0.955	0.431		
S_U.rs1	V_{max}	S_U	2	15.532	1.91×10^{-7}	subject	55.139
						residual	66.567

Table 2. Statistical analysis of the influence of spatial and temporal uncertainties and their interaction on saccadic latency and V_{max}. A LMM model was fitted using the restricted maximum likelihood method and statistics were calculated using Type III ANOVA with Satterthwaite's method. *df* degrees of freedom, *σ* SD of the random terms (subject and residual).

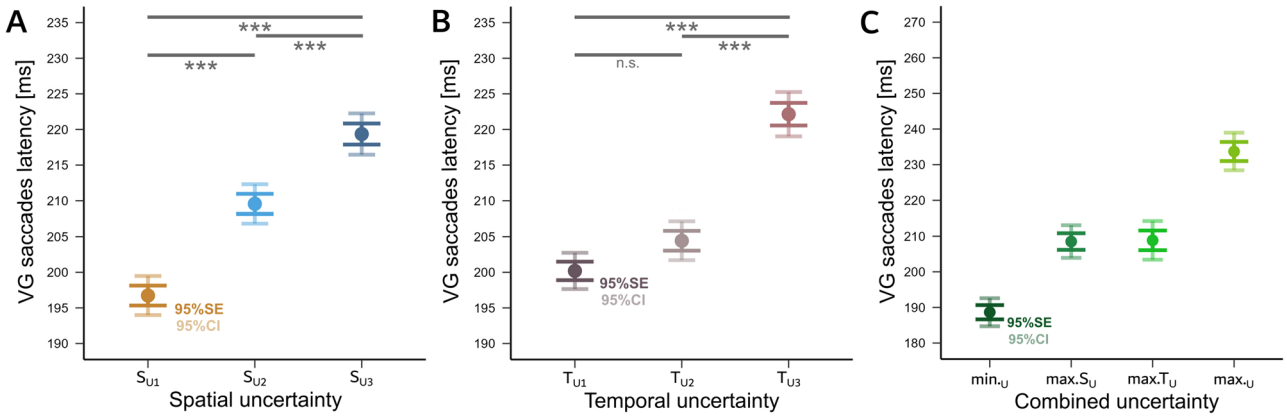

Figure 3. Latency of visually-guided saccades for different levels of temporal and spatial uncertainty. Average saccade latency (*dot*) for different levels of spatial (**A**), temporal (**B**) and combined uncertainty (**C**). For combined uncertainty, only the general trend will be presented given that this variable was created a posteriori and that no planned comparisons could therefore be performed. *Whiskers* represent standard error (95% SE) and confidence intervals (95% CI). *Horizontal black lines* indicate post-hoc significance between factor levels. *n.s.* not significant, *p < 0.01, **p < 0.001, ***p < 0.0001.

The experimental paradigm also included catch trials that were used to keep subjects motivated and attentive. The analysis of saccadic latency in catch trials can be found in the Supplementary Material section (see Supplementary Table S4 as well as Supplementary Fig. S2 online).

Maximum eye velocity during movement execution

A similar LMM pipeline was applied to the V_{max} of the eye during the saccade towards the IS. Of all tested models, the 'S_U.rs1' model including only the effect of spatial uncertainty was best fitting the data (see Supplementary Table S1 online). The LMM analysis included 44 ± 13 saccadic V_{max} recordings per subject in S_{U1}, 47 ± 13 in S_{U2} and 46 ± 13 in S_{U3} condition. Saccadic V_{max} decreased together with increasing spatial uncertainty ($p = 1.91 \times 10^{-7}$, see model S_U.rs1 in Table 2). Post-hoc Tukey comparisons showed that V_{max} significantly decreased between S_{U1} and S_{U3} ($p = 7.90 \times 10^{-8}$) and S_{U2} and S_{U3} levels ($p = 0.006$, see Supplementary Table S5 online). The LMM analysis

included 41 ± 13 saccadic V_{max} recordings per subject in T_{U1}, 46 ± 14 in T_{U2} and 44 ± 12 in T_{U3} condition. There was however no effect of temporal uncertainty (model 'T_U.rs1', p = 0.469). Here also, no interaction between spatial and temporal uncertainty was found (model 'full.rs1', p = 0.431, see Table 2). The V_{max} of visually-guided saccades was the largest when in the condition without experimental spatial uncertainty (see Fig. 4A) but remained independent from temporal uncertainty levels (see Fig. 4B).

The analysis of V_{max} during catch trials can be found in the Supplementary Material (see Supplementary Table S6 as well as Supplementary Fig. S3 online).

Discussion

In the present study, the influences of expected spatial and temporal uncertainty on movement preparation and execution were estimated. We tested the hypothesis that the two types of uncertainty could interact (or not) and have a different impact during these two periods. Eye movements were used as operant responses, given their known sensitivity to spatiotemporal variables and higher order cognitive factors.

We found that during the FP, pupil dilation was significantly modulated by expected temporal uncertainty *only* and maximal for the higher level of T_U. This observation suggests that subjects retrieved from memory the association between the star-like cue and the probability distribution of the IS[45]. Previous studies in decision-making indicated that increased pupil dilation could correspond to higher cued uncertainty ([46–48] but see[49]) and higher expected task difficulty[50]. In the current study, a higher difficulty to predict the onset of the IS could be associated with the T_{U3} condition, therefore causing a larger pupil dilation. However, a more parsimonious interpretation would be to suggest that subjects prepared to the earliest possible appearance of the IS. Given that pupil dilation controls the amount of light that enters the eye and therefore the sensitivity of the visual system to detect stimuli[33], a stronger pupil dilation could be achieved in expectation of a stimulus that could appear earlier. Indeed, the temporal cue did not provide information about exact FP length but only informed about its kurtosis. Given that the T_{U3} cue indicated that the IS could appear as early as 975 ms after WS offset (see Fig. 1), an early increase in pupil size could occur. This is also in agreement with Akdoğan et al.[27] who showed that the pupil could dilate earlier when the attended target could be expected sooner. An increase of pupil size in anticipation of a stimulus with lower temporal certainty was also observed by Shalev and Nobre[51]. It was interpreted as an adaptation of the level of arousal of experimental subjects to the experimental context where the ISI was either fixed, or variable.

At the end of the variable foreperiod, the imperative stimulus evoked a saccadic eye movement to the 'placer' where the target appeared. We found that the latency of these visually-guided saccades was lengthened with both increasing spatial and temporal uncertainty. No statistical interaction between factors (S_U and T_U) was detected but exploratory analyses using $Comb_U$ suggest an additive effect of both types of uncertainty. Furthermore, spatial uncertainty (but *not* temporal uncertainty) affected V_{max} (see Fig. 4B). V_{max} was previously reported to change based on mental fatigue[52], arousal[53,54], reward[55,56], intrinsic value[57] and economic utility[58]. Here, we show that it could covary with expected spatial but not temporal uncertainty. It could be suggested that during movement execution, temporal information was no longer relevant. Indeed, temporal information could be crucial when the timing of the movement has to be prepared and manifests itself on movement latency. However, there was no constraint to precisely time the saccade to the position where the target was briefly presented. Therefore, temporal information was not relevant to gaze at the final position of the IS. The position of the IS could be represented in the premotor map present in the deeper layers of the superior colliculus (SC). It has been shown that spatial uncertainty could alter the representation of the saccade goal on this collicular map[61] and that saccadic V_{max} could be modulated by variation of neural activity in the SC[59,60]. Therefore, we suggest that spatial uncertainty could alter V_{max} by modulating neural activity at the locus of SC activation.

Figure 5 shows a schematic representation of statistical effects on behavioral responses during the different steps of the task in the present study. During target expectation, only temporal uncertainty modulated pupil

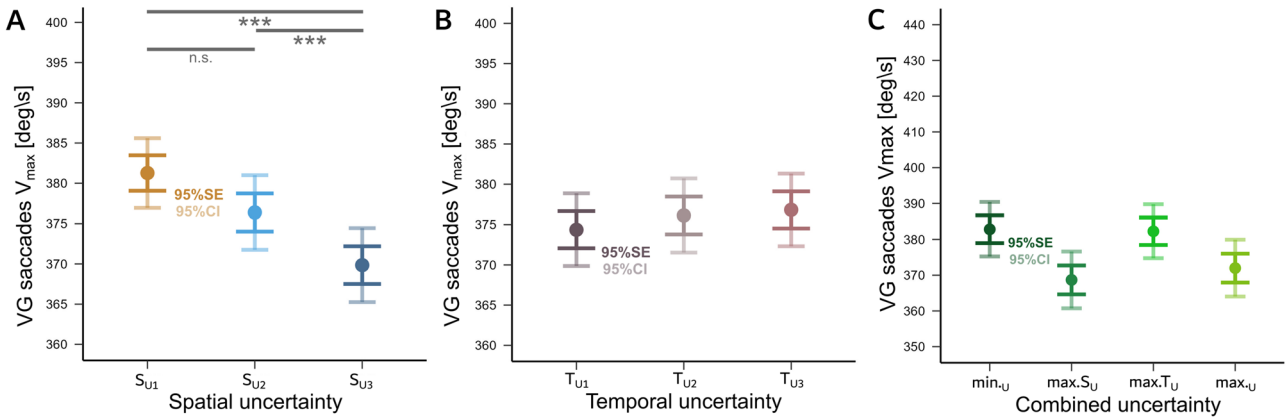

Figure 4. Average V_{max} of visually-guided saccades for different levels of spatial (**A**) temporal (**B**) and combined uncertainty (**C**). *Whiskers* represent standard error (95% SE) and confidence intervals (95% CI) of the mean. *Horizontal black lines* indicate post-hoc significance between factor levels. *n.s.* not significant, *p < 0.01, **p < 0.001, ***p < 0.0001. For combined uncertainty, only the general trend is presented.

Figure 5. Schematic representation of the influence of temporal and spatial uncertainties on oculomotor measures and pupillary response during the task. During the foreperiod, only temporal expectancy (T_U) of the IS increased pupil dilation. After IS onset, both types of uncertainty were altering saccadic latency. Once the saccade was initiated, only spatial uncertainty (S_U) influenced its maximum velocity (V_{max}). Abbreviations: n.s. not significant, *** $p < 0.0001$.

size. After IS appearance, saccadic latency increased with both uncertainties. However, movement *execution* was affected only by spatial uncertainty.

We suggest that there could be a prioritization of the most relevant information at different steps during the task. Indeed, during the FP temporal preparation was more relevant and spatial uncertainty had no significant effect. This could explain the discrepancy with previous results where an influence of expected spatial uncertainty on pupil dilation was observed in a context without temporal uncertainty[22].

During the FP, spatial uncertainty was downplayed but the cue could have been stored in working memory. This independence of temporal and spatial expectations are in contrast to what was suggested based on results obtained in a visual orientation discrimination task by Rohenkohl et al.[31]. However, this could be related to the use of a simple reaction time task in the present study[32]. Indeed, the potential spatiotemporal interaction could depend on the task at hand and not occur in simple RT tasks[62,63]. After the appearance of the IS but before saccade onset, a lingering temporal expectation and a (now) relevant spatial uncertainty probably added their effects. Indeed, the content of spatial working memory (expected spatial uncertainty) was retrieved and altered saccadic latency. Finally, the modulation of V_{max} exclusively by spatial uncertainty shows that temporal information was not relevant during movement execution. Indeed, the target had been briefly displayed previously and estimating its timing based on prior information was therefore not necessary any more.

It could be suggested that the memorization and use of the temporal uncertainty cue during the FP was associated with a greater mental effort than for the spatial cue. Therefore, pupil dilation was larger in the T_U conditions. It has been shown previously that human subjects can learn different types of probability distributions if they are associated with an explicit cue[64]. However, it cannot be ruled out that this is more demanding than in the spatial domain. Concerning the influence of the $Comb_U$ variable, it should be stressed that it provides some interesting insights for future experiments. However, this variable was created *a posteriori*, and it was not designed as an independent factor beforehand (see[65]). Therefore, the interpretation of the impact of $Comb_U$ is limited but suggests that in extreme cases, there could be an interaction between factors. Nevertheless, we cannot statistically support this statement.

In conclusion, results of the present study illustrate how the brain could flexibly use spatiotemporal 'known unknowns' as a function of task context.

Data availability

The datasets generated during and/or analyzed during the current study are available from the corresponding author on reasonable request.

Received: 8 March 2024; Accepted: 22 July 2024
Published online: 30 July 2024

References

1. Teufel, C. & Fletcher, P. C. Forms of prediction in the nervous system. *Nat. Rev. Neurosci.* **21**(4), 231–242 (2020).
2. Matthews, W. J. & Meck, W. H. Temporal cognition: Connecting subjective time to perception, attention, and memory. *Psychol. Bull.* **142**(8), 865–907 (2016).
3. Summerfield, C. & Egner, T. Expectation (and attention) in visual cognition. *Trends Cogn. Sci.* **13**, 403–409 (2009).
4. Bach, D. R. & Dolan, R. J. Knowing how much you don't know: A neural organization of uncertainty estimates. *Nat. Rev. Neurosci.* **13**(8), 572–586 (2012).
5. Catena, A. *et al.* The brain network of expectancy and uncertainty processing. *PLoS ONE* **7**(7), e40252 (2012).
6. Woodrow, H. The measurement of attention. *Psychol. Monogr.* **17**, 1–158 (1914).
7. Niemi, P. & Naatanen, R. Foreperiod and simple reaction time. *Psychol. Bull.* **89**(1), 133–162 (1981).
8. Salet, J. M., Kruijne, W. & Van Rijn, H. Implicit learning of temporal behavior in complex dynamic environments. *Psychon. Bull. Rev.* **28**(4), 1270–1280 (2021).
9. Los, S. A., Kruijne, W. & Meeter, M. Hazard versus history: Temporal preparation is driven by past experience. *J. Exp. Psychol. Hum. Percept. Perform.* **43**, 78–88 (2017).

10. Trillenberg, P., Verleger, R., Wascher, E., Wauschkuhn, B. & Wessel, K. Cnv and temporal uncertainty with 'ageing' and 'non-ageing' s1–s2 intervals. *Clin. Neurophysiol.* **111**(7), 1216–1226 (2000).
11. Gottsdanker, R. The attaining and maintaining of preparation. In *Attention and Performance* (eds Rabbit, P. & Dornic, S.) 33–49 (Academic Press, 1975).
12. Vallesi, A. & Shallice, T. Developmental dissociations of preparation over time: Deconstructing the variable foreperiod phenomena. *J. Exp. Psychol. Hum. Percept. Perform.* **33**(6), 1377–1388 (2007).
13. Vangkilde, S., Coull, J. T. & Bundesen, C. Great expectations: Temporal expectation modulates perceptual processing speed. *J. Exp. Psychol. Hum. Percept. Perform.* **38**(5), 1183–1191 (2012).
14. Vangkilde, S., Petersen, A. & Bundesen, C. Temporal expectancy in the context of a theory of visual attention. *Philos. Trans. R. Soc. Lond. B. Biol. Sci.* **368**(1628), 20130054 (2013).
15. Janssen, P. & Shadlen, M. N. A representation of the hazard rate of elapsed time in macaque area lip. *Nat. Neurosci.* **8**(2), 234–241 (2005).
16. de Hemptinne, C., Nozaradan, S., Duvivier, Q., Lefevre, P. & Missal, M. How do primates anticipate uncertain future events?. *J. Neurosci.* **27**(16), 4334–4341 (2007).
17. Ameqrane, I., Pouget, P., Wattiez, N., Carpenter, R. & Missal, M. Implicit and explicit timing in oculomotor control. *PLoS ONE* **9**(4), e93958 (2014).
18. Degos, B., Ameqrane, I., Rivaud-Péchoux, S., Pouget, P. & Missal, M. Short-term temporal memory in idiopathic and parkin-associated parkinson's disease. *Sci. Rep.* **8**(1), 7637 (2018).
19. Hsu, T. Y., Lee, H. C., Lane, T. J. & Missal, M. Temporal preparation, impulsivity and short-term memory in depression. *Front. Behav. Neurosci.* **13**, 258 (2019).
20. Oswal, A., Ogden, M. & Carpenter, R. H. S. The time course of stimulus expectation in a saccadic decision task. *J. Neurophysiol.* **97**(4), 2722–2730 (2007).
21. Degos, B., Pouget, P. & Missal, M. From anticipation to impulsivity in parkinson's disease. *Npj Parkinson's Dis.* **8**(1), 125 (2022).
22. Drążyk, D. & Missal, M. The oculomotor signature of expected surprise. *Sci. Rep.* **12**(1), 2543 (2022).
23. Coull, J. T. & Nobre, A. C. Where and when to pay attention: The neural systems for directing attention to spatial locations and to time intervals as revealed by both pet and fmri. *J. Neurosci.* **18**(18), 7426–7435 (1998).
24. Griffin, I. C., Miniussi, C. & Nobre, A. C. Multiple mechanisms of selective attention: Differential modulation of stimulus processing by attention to space or time. *Neuropsychologia* **40**(13), 2325–2340 (2002).
25. Nobre, A. C. Orienting attention to instants in time. *Neuropsychologia* **39**(12), 1317–1328 (2001).
26. Rolke, B. & Hofmann, P. Temporal uncertainty degrades perceptual processing. *Psychon. Bull. Rev.* **14**(3), 522–526 (2007).
27. Akdoğan, B., Balcı, F. & Van Rijn, H. Temporal expectation indexed by pupillary response. *Timing Time Percept.* **4**(4), 354–370 (2016).
28. Preuschoff, K., Hart, B. M. & Einhauser, W. Pupil dilation signals surprise: Evidence for noradrenaline's role in decision making. *Front. Neurosci.* **5**, 115 (2011).
29. Lavín, C., San Martín, R. & Rosales-Jubal, E. Pupil dilation signals uncertainty and surprise in a learning gambling task. *Front. Behav. Neurosci.* **7**, 218 (2014).
30. Wagemans, J. *et al.* Century of gestalt psychology in visual perception: I. perceptual grouping and figure-ground organization. *Psychol. Bull.* **138**(6), 1172–1217 (2012).
31. Rohenkohl, G., Gould, I. C., Pessoa, J. & Nobre, A. C. Combining spatial and temporal expectations to improve visual perception. *J. Vis.* **14**(4), 8 (2014).
32. Tal-Perry, N. & Yuval-Greenberg, S. The spatiotemporal link of temporal expectations: Contextual temporal expectation is independent of spatial attention. *J. Neurosci.* **42**(12), 2516–2523 (2022).
33. Mathôt, S. Pupillometry: Psychology, physiology, and function. *J. Cogn.* **1**(1), 16 (2018).
34. Kyröläinen, A., Porretta, V., van Rij, J. & Järvikivi, J. *PupilPre: Tools for Preprocessing Pupil Size Data. Version 0.6.2*. Documentation at: https://CRAN.R-project.org/package=PupilPre (2019)
35. Mathôt, S, Fabius, J, Van Heusden, E. & Van der Stigchel, S. Safe and sensible preprocessing and baseline correction of pupil-size data. *Behav. Res. Methods* **50(1)**, 94–106 (2018).
36. Maris, E. & Oostenveld, R. Nonparametric statistical testing of eeg- and meg-data. *J. Neurosci. Methods* **164**, 177–190 (2007).
37. Voeten, C. C. *Permutes: Permutation Tests for Time Series Data. Version 2.8*. Documentation at: https://cran.r-project.org/web/packages/permutes/permutes.pdf (2023).
38. Sassenhagen, J. & Draschkow, D. Cluster-based permutation tests of meg/eeg data do not establish significance of effect latency or location. *Psychophysiology* **56**(6), e13335 (2019).
39. Fox, J. & Weisberg, S. *An R Companion to Applied Regression* 3rd edn. (Sage, 2019).
40. Bates, D., Mächler, M., Bolker, B. & Walker, S. Fitting linear mixed-effects models using lme4. *J. Stat. Softw.* **67**(1), 1–48 (2015).
41. Lüdecke, D., Ben-Shachar, M. S., Patil, I., Waggoner, P. & Makowski, D. Performance: An r package for assessment, comparison and testing of statistical models. *J. Open Source Softw.* **6**, 3139 (2021).
42. Barr, D. J., Levy, R., Scheepers, C. & Tily, H. J. Random effects structure for confirmatory hypothesis testing: Keep it maximal. *J. Mem. Lang.* **68**(3), 255–278 (2013).
43. Zuur, A. F., Ieno, E. N., Walker, N., Saveliev, A. A. & Smith, G. M. *Mixed Effects Models and Extensions in Ecology with R* (Springer, 2009).
44. Bolker, B. M. *et al.* Generalized linear mixed models: A practical guide for ecology and evolution. *Trends Ecol. Evol.* **24**(3), 127–135 (2009).
45. Los, S. A. *et al.* The warning stimulus as retrieval cue: The role of associative memory in temporal preparation. *Cogn. Psychol.* **125**, 101378 (2021).
46. Satterthwaite, T. D. *et al.* Dissociable but inter-related systems of cognitive control and reward during decision making: Evidence from pupillometry and event-related fmri. *Neuroimage* **37**(3), 1017–1031 (2007).
47. Geng, J. J., Blumenfeld, Z., Tyson, T. L. & Minzenberg, M. J. Pupil diameter reflects uncertainty in attentional selection during visual search. *Front. Hum. Neurosci.* **9**, 435 (2015).
48. de Berker, A. O. *et al.* Computations of uncertainty mediate acute stress responses in humans. *Nat. Commun.* **7**(1), 10996 (2016).
49. Cavanagh, J. F., Wiecki, T. V., Kochar, A. & Frank, M. J. Eye tracking and pupillometry are indicators of dissociable latent decision processes. *J. Exp. Psychol.* **143**(4), 1476–1488 (2014).
50. Irons, J. L., Jeon, M. & Leber, A. B. Pre-stimulus pupil dilation and the preparatory control of attention. *PLoS ONE* **12**(12), e0188787 (2017).
51. Shalev, N. & Nobre, A. C. Eyes wide open: Regulation of arousal by temporal expectations. *Cognition* **224**, 105062 (2022).
52. Bachurina, V. & Arsalidou, M. Multiple levels of mental attentional demand modulate peak saccade velocity and blink rate. *Heliyon* **8**(1), e08826 (2022).
53. di Girolamo, G. J., Patel, N. & Blaukopf, C. L. Arousal facilitates involuntary eye movements. *Exp. Brain Res.* **234**(7), 1967–1976 (2016).
54. di Stasi, L. L., Catena, A., Cañas, J. J., Macknik, S. L. & Martinez-Conde, S. Saccadic velocity as an arousal index in naturalistic tasks. *Neurosci. Biobehav. Rev.* **37**(5), 968–975 (2013).
55. Manohar, S. G. & Husain, M. Human ventromedial prefrontal lesions alter incentivisation by reward. *Cortex* **76**, 104–120 (2016).

56. Muhammed, K., Dalmaijer, E., Manohar, S. & Husain, M. Voluntary modulation of saccadic peak velocity associated with individual differences in motivation. *Cortex* **122**, 198–212 (2020).
57. Haith, A. M., Reppert, T. R. & Shadmehr, R. Evidence for hyperbolic temporal discounting of reward in control of movements. *J. Neurosci.* **32**(34), 11727–11736 (2012).
58. Shadmehr, R., Reppert, T. R., Summerside, E. M., Yoon, T. & Ahmed, A. A. Movement vigor as a reflection of subjective economic utility. *Trends Neurosci.* **42**(5), 323–336 (2019).
59. Smalianchuk, I., Jagadisan, U. K. & Gandhi, N. J. Instantaneous midbrain control of saccade velocity. *J. Neurosci.* **38**(47), 10156–10167 (2018).
60. Wolf, C. & Lappe, M. Vision as oculomotor reward: Cognitive contributions to the dynamic control of saccadic eye movements. *Cogn. Neurodyn.* **15**(4), 547–568 (2021).
61. Basso, M. A. & Wurtz, R. H. Modulation of neuronal activity by target uncertainty. *Nature* **389**(6646), 66–69 (1997).
62. van Ede, F., Rohenkohl, G., Gould, I. & Nobre, A. C. Purpose-dependent consequences of temporal expectations serving perception and action. *J. Neurosci.* **40**(41), 7877–7886 (2020).
63. Weinbach, N., Shofty, I., Gabay, S. & Henik, A. Endogenous temporal and spatial orienting: Evidence for two distinct attentional mechanisms. *Psychon. Bull. Rev.* **22**, 967–973 (2015).
64. Mattiesing, R. M., Kruijne, W., Meeter, M. & Los, S. A. Timing a week later: The role of long-term memory in temporal preparation. *Psychon. Bull. Rev.* **24**(6), 1900–1905 (2017).
65. Palmieri, H. & Carrasco, M. Task demand mediates the interaction of spatial and temporal attention. *Sci. Rep.* **14**, 9228 (2024).

Acknowledgements

This work was supported by the Fonds de la Recherche Scientifique—FNRS under Grant No CDR/OL J0132.21. Marcus Missal is a Professor at the Université catholique de Louvain. Dominika Drążyk is a Research Fellow at the Fonds de la Recherche Scientifique—FNRS. Authors wish to thank Sébastien Forest for the title of the paper.

Author contributions

A.B., M.M. and D.D. conceived the experiment, A.B. conducted the experiment, A.B., M.M. and D.D. analyzed the results. All authors reviewed the manuscript.

Competing interests

The authors declare no competing interests.

Additional information

Supplementary Information The online version contains supplementary material available at https://doi.org/10.1038/s41598-024-68233-w.

Correspondence and requests for materials should be addressed to M.M.

Reprints and permissions information is available at www.nature.com/reprints.

Publisher's note Springer Nature remains neutral with regard to jurisdictional claims in published maps and institutional affiliations.

Open Access This article is licensed under a Creative Commons Attribution-NonCommercial-NoDerivatives 4.0 International License, which permits any non-commercial use, sharing, distribution and reproduction in any medium or format, as long as you give appropriate credit to the original author(s) and the source, provide a link to the Creative Commons licence, and indicate if you modified the licensed material. You do not have permission under this licence to share adapted material derived from this article or parts of it. The images or other third party material in this article are included in the article's Creative Commons licence, unless indicated otherwise in a credit line to the material. If material is not included in the article's Creative Commons licence and your intended use is not permitted by statutory regulation or exceeds the permitted use, you will need to obtain permission directly from the copyright holder. To view a copy of this licence, visit http://creativecommons.org/licenses/by-nc-nd/4.0/.

© The Author(s) 2024